Koiter-Based Solution for the Initial Post-buckling Behavior of Moderately Thick Orthotropic and Shear Deformable Cylindrical Shells Under External Pressure

G. A. Kardomateas
Professor,
School of Aerospace Engineering,
Georgia Institute of Technology,
Atlanta, GA 30332-0150

The initial post-buckling behavior of moderately thick orthotropic shear deformable cylindrical shells under external pressure is studied by means of Koiter's general post-buckling theory. To this extent, the objective is the calculation of imperfection sensitivity by relating to the initial post-buckling behavior of the perfect structure, since it is generally recognized that the presence of small geometrical imperfections in some structures can lead to significant reductions in their buckling strengths. A shear deformation theory, which accounts for transverse shear strains and rotations about the normal to the shell midsurface, is employed to formulate the shell equations. The initial post-buckling analysis indicates that for several combinations and geometric dimensions, the shell under external pressure will be sensitive to small geometrical imperfections and may buckle at loads well below the bifurcation predictions for the perfect shell. On the other hand, there are extensive ranges of geometrical dimensions for which the shell is insensitive to imperfections, and, therefore it would exhibit stable post-critical behavior and have a load-carrying capacity beyond the bifurcation point. The range of imperfection sensitivity depends strongly on the material anisotropy, and also on the shell thickness and whether the end pressure loading is included or not. For example, for the circumferentially reinforced graphite/epoxy example case studied, it was found that the structure is not sensitive to imperfections for values of the Batdorf length parameter $\bar{z}$ above $\simeq 270$, whereas for the axially reinforced case the structure is imperfection-sensitive even at the high range of length values; for the isotropic case, the structure is not sensitive to imperfections above $\bar{z} \simeq 1000$.

Introduction

Recent studies on the buckling of moderately thick orthotropic shells under external pressure have pointed to the importance of the effects of orthotropy and thickness in lowering the critical load and rendering classical shell theory estimates, in some cases quite non-conservative, in comparison to isotropic thin shell construction (e.g., Kardomateas, 1993; Kardomateas and Chung, 1994; Simitses et al., 1993). It is natural to consider next the extent to which these effects influence the imperfection sensitivity of the shell.

This can be achieved in an efficient manner by applying Koiter's (1945, 1963) general post-buckling theory, according to which, the slope of the secondary curve and the degradation of the critical loads with imperfections are described by means of the value and sign of the coefficient of the post-buckled state, b. A comprehensive survey by Hutchinson and Koiter (1970) provides a very useful bibliography, together with an overview of the achievements and goals of this theory. In addition to Koiter's original work, several papers have produced variations of the theory with a bias towards virtual work (Budiansky and Hutchinson, 1964; Budiansky, 1974).

The other approach to calculating the imperfection sensitivity is the formulation and solution of the full nonlinear imperfect shell problem. A solution methodology for the analysis of an isotropic, geometrically imperfect, thin, circular cylindrical shell loaded by uniform axial compression, based on the Galerkin procedure, was described by Sheinman and Simitses (1983).

Regarding applications of Koiter's theory to shells, several papers have been published, mostly based on isotropic classical thin shell formulations (e.g., Hutchinson, 1968). Hutchinson and Frauenthal (1969) studied the post-buckling and imperfection sensitivity of stringer reinforced cylindrical shells. Regarding external pressure loading, Budiansky and Amazigo (1968) studied an isotropic thin shell under hydrostatic pressure on the basis of the nonlinear Kármán-Donnell theory and found that these shells may be sensitive to imperfections in some instances and insensitive in others. Also, a much earlier post-buckling shell analysis was made by Koiter (1956) on the basis of his general formulation in terms of displacements.

The purpose of the present paper is to extend these earlier studies on the initial post-buckling behavior by including material orthotropy and basing the analysis on a shear deformation shell theory rather than a classical Donnell-based formulation. This is because the construction of the shell structure involves

Contributed by the Applied Mechanics Division of THE AMERICAN SOCIETY OF MECHANICAL ENGINEERS for publication in the ASME JOURNAL OF APPLIED MECHANICS.

Discussion on the paper should be addressed to the Technical Editor, Professor Lewis T. Wheeler, Department of Mechanical Engineering, University of Houston, Houston, TX 77204-4792, and will be accepted until four months after final publication of the paper itself in the ASME JOURNAL OF APPLIED MECHANICS.

Manuscript received by the ASME Applied Mechanics Division, Aug. 21, 1996; final revision, Mar. 22, 1997. Associate Technical Editor: S. Kryiakides.

advanced composite materials and moderate shell wall thickness where shear effects are more pronounced rendering classical shell theories inadequate. Besides the anisotropy, composite shells have most often one other important distinguishing feature, namely extensional-to-shear modulus ratio much larger than that of their metal counterparts.

In this regard, several improved shell theories have been formulated (e.g., Naghdi and Cooper, 1956; Mirsky and Herrmann, 1957; Dong and Tso, 1972; Whitney and Sun, 1974; Reddy and Liu, 1985). Most of these refined theories focused on their application to vibration problems and can be categorized into two basic groups: one with in-plane displacements approximated by linear variations in the thickness direction and the other by cubic polynomials. The first group requires the so-called shear correction factors as first suggested by Mindlin (1951) for homogeneous isotropic plates to account for the nonuniform distribution of transverse shear stresses and strains across the thickness. The second group, also called higher-order theories, uses higher-order approximations for shear stresses and strains and does not use shear correction factors but calls for a more involved analysis. The present paper is based on the simpler Timoshenko-Mindlin kinematic hypothesis with shear correction factors. Although the formulation reduces in general to the numerical solution of a standard two-point boundary value problem for ordinary differential equations, a simple closed-form solution can be derived by considering the limit of a very long cylindrical shell. It should also be mentioned that an orthotropic ring under external pressure does not exhibit imperfection sensitivity (Fu and Waas, 1995). It will be shown in this paper that an orthotropic shell under external pressure has wide ranges of length in which it is imperfection sensitive, and these ranges depend on the anisotropy of the material.

Basic Equations

Consider an orthotropic circular cylindrical shell of thickness h, mean radius R, and length l. The shell is referred to a coordinate system x, θ, and z, in which x and θ are in the axial and circumferential directions of the shell and z is in the direction of the outward normal to the middle surface. The corresponding displacements at the middle surface are designated by u, v, and w and the rotations of a normal to the middle surface in the θz and xz-planes respectively are denoted by ϕ and ψ. The nonlinear strain-displacement relations are

$$\epsilon_x = u_{,x} + \tfrac{1}{2}w_{,x}^2, \tag{1a}$$

$$\epsilon_\theta = \frac{v_{,\theta} + w}{R} + \frac{1}{2R^2}\, w_{,\theta}^2, \tag{1b}$$

$$\gamma_{x\theta} = v_{,x} + \frac{u_{,\theta}}{R} + \frac{1}{R}\, w_{,x}w_{,\theta}, \tag{1c}$$

$$\gamma_{\theta z} = \phi + \frac{w_{,\theta}}{R}\,; \quad \gamma_{xz} = \psi + w_{,x}, \tag{1d}$$

and the bending strains (or curvature) relationships are

$$\kappa_x = \psi_{,x}; \quad \kappa_\theta = \frac{\phi_{,\theta}}{R}\,; \quad \kappa_{x\theta} = \phi_{,x} + \frac{\psi_{,\theta}}{R}\,. \tag{1e}$$

Notice that based on the Timoshenko-Mindlin kinematic hypothesis, the displacement field $\bar{u}$, $\bar{v}$, $\bar{w}$ at an arbitrary point, is represented by

$$\bar{u}(x, \theta, z) = u(x, \theta) + z\psi(x, \theta), \tag{2a}$$

$$\bar{v}(x, \theta, z) = v(x, \theta) + z\phi(x, \theta), \tag{2b}$$

$$\bar{w}(x, \theta, z) = w(x, \theta). \tag{2c}$$

In these equations, a comma denotes differentiation with respect to the corresponding coordinate; ϵ_x, ϵ_θ, and $\gamma_{x\theta}$ are the inplane strains; $\gamma_{\theta z}$ and γ_{xz} are transverse shear strains. Notice that for the classical shell theory, $\psi = -w_{,x}$ and $\phi = -w_{,\theta}/R$, therefore $\gamma_{xz} = \gamma_{\theta z} = 0$.

One thing should be mentioned at this point. The shallow classical shell theory equations were chosen because of their simplicity and for the desire to stay with the simplest possible shell formulation for purposes of clarity of the presentation of the initial post-buckling behavior. Although the classical shallow shell theory has been shown to provide poor accuracy for low n (e.g., Brush and Almroth, 1975), this paper employs a shear deformable theory, and for this case it has been shown with a few examples (Kardomateas and Philobos, 1995) that the first-order shear deformation theory ($n = 2$) gives critical loads very close to the three-dimensional elasticity solution, although the classical shell theory would give, for these examples, critical loads noticably above the elasticity ones.

Asymptotic Expansions for the Post-buckling Behavior of the Perfect Shell. In the post-critical regime, the structure suffers deviations in the displacement profile from the buckling mode $\mathbf{V}_1 = \{u^{(1)}, v^{(1)}, w^{(1)}\}$, and simultaneously, p will deviate from p_c, the critical pressure. Define $\eta = p/p_c$. Then, the displacements of the structure in the initial post-buckling phase can be written as

$$\mathbf{V} = \eta\mathbf{V}_0 + \xi\mathbf{V}_1 + \xi^2\mathbf{V}_2 + \xi^3\mathbf{V}_3 + \xi^4\mathbf{V}_4 + \ldots \tag{3a}$$

where η depends on ξ. In this expansion $\mathbf{V}_0$ is associated with the prebuckling state, $\mathbf{V}_1$ describe a normalized buckling mode, and the remaining terms are orthogonal to the buckling mode. For example,

$$u = \eta u_0 + \xi u^{(1)} + \xi^2 u^{(2)} + \xi^3 u^{(3)} + \xi^4 u^{(4)} + \ldots. \tag{3b}$$

Also, similar expansions are assumed for the resultant forces and moments. For example,

$$N_x = \eta N_{x0} + \xi N_x^{(1)} + \xi^2 N_x^{(2)} + \xi^3 N_x^{(3)} + \xi^4 N_x^{(4)} + \ldots. \tag{3c}$$

Substituting into the nonlinear strain displacement Eqs. (1) give the strains in the form

$$\epsilon_{ij} = \eta\epsilon_{ij}^0 + \xi\epsilon_{ij}^{(1)} + \xi^2\epsilon_{ij}^{(2)} + \xi^3\epsilon_{ij}^{(3)} + \xi^4\epsilon_{ij}^{(4)} + \ldots. \tag{3d}$$

Second-Order Strains. In the following we shall use e_{ij} to denote the linear strains, for example $e_x = u_{,x}$.

Using the asymptotic expansion (3) and the nonlinear strain-displacement relations (1) gives the second-order strains in the abbreviated form:

$$\epsilon^{(2)} = e^{(2)} + L(\mathbf{V}_1). \tag{4a}$$

Specifically, the second-order normal strains are

$$\epsilon_x^{(2)} = u_{,x}^{(2)} + L_x(\mathbf{V}_1); \quad \epsilon_\theta^{(2)} = \frac{v_{,\theta}^{(2)} + w^{(2)}}{R} + L_\theta(\mathbf{V}_1)\,, \tag{4b}$$

where

$$L_x(\mathbf{V}_1) = \frac{1}{2}\, w_{,x}^{(1)2}\,; \quad L_\theta(\mathbf{V}_1) = \frac{1}{2R^2}\, w_{,\theta}^{(1)2}. \tag{4c}$$

The second-order shear strains are

$$\gamma_{x\theta}^{(2)} = v_{,x}^{(2)} + \frac{u_{,\theta}^{(2)}}{R} + L_{x\theta}(\mathbf{V}_1), \tag{5a}$$

$$\gamma_{\theta z}^{(2)} = \phi^{(2)} + \frac{w_{,\theta}^{(2)}}{R}\,; \quad \gamma_{xz}^{(2)} = \psi^{(2)} + w_{,x}^{(2)}, \tag{5b}$$

$$L_{x\theta}(\mathbf{V}_1) = \frac{1}{R} w_{,x}^{(1)} w_{,\theta}^{(1)}; \quad L_{\theta z}(\mathbf{V}_1) = L_{xz}(\mathbf{V}_1) = 0. \quad (5c)$$

The third or fourth-order strains can be found in a similar fashion.

Stress Resultants. In the first-order shear deformation shell theory considered, the generalized stress σ consists of the five force resultants N_x, N_θ, $N_{x\theta}$, Q_{xz}, and $Q_{\theta z}$ and the three moment resultants M_x, M_θ, and $M_{x\theta}$. The generalized strain ϵ represents the five membrane strains ϵ_x, ϵ_θ, $\gamma_{x\theta}$, γ_{xz}, $\gamma_{\theta z}$ and the three bending strains κ_x, κ_θ, and $\kappa_{x\theta}$. The generalized displacement consists of the five midpoint linear and angular displacements u, v, w, ϕ, and ψ.

For orthotropy, the stress resultants are related to the strain components by

$$\sigma = \begin{bmatrix} N_x \\ N_\theta \\ Q_{\theta z} \\ Q_{xz} \\ N_{x\theta} \\ M_x \\ M_\theta \\ M_{x\theta} \end{bmatrix} = \begin{bmatrix} c_{11} & c_{12} & 0 & 0 & 0 & 0 & 0 & 0 \\ c_{12} & c_{22} & 0 & 0 & 0 & 0 & 0 & 0 \\ 0 & 0 & k_2^2 c_{44} & 0 & 0 & 0 & 0 & 0 \\ 0 & 0 & 0 & k_1^2 c_{55} & 0 & 0 & 0 & 0 \\ 0 & 0 & 0 & 0 & c_{66} & 0 & 0 & 0 \\ 0 & 0 & 0 & 0 & 0 & D_{11} & D_{12} & 0 \\ 0 & 0 & 0 & 0 & 0 & D_{12} & D_{22} & 0 \\ 0 & 0 & 0 & 0 & 0 & 0 & 0 & D_{66} \end{bmatrix} \times \begin{bmatrix} \epsilon_x \\ \epsilon_\theta \\ \gamma_{\theta z} \\ \gamma_{xz} \\ \gamma_{x\theta} \\ \kappa_x \\ \kappa_\theta \\ \kappa_{x\theta} \end{bmatrix} = C.\epsilon, \quad (6a)$$

where c_{ij} are the stiffness constants (we have used the notation $1 \equiv x$ (axial), $2 \equiv \theta$, $3 \equiv z$ (radial), $4 \equiv \theta z$, $5 \equiv xz$ and $6 \equiv x\theta$) and k_1^2, k_2^2 are the shear correction factors. These constants are expressed in terms of the moduli and Poisson's ratios of the material and the thickness h of the shell as follows:

$$c_{11} = \frac{hE_x}{1 - \nu_{x\theta}\nu_{\theta x}}; \quad c_{12} = \frac{h\nu_{x\theta}E_\theta}{1 - \nu_{x\theta}\nu_{\theta x}}; \quad c_{22} = \frac{hE_\theta}{1 - \nu_{x\theta}\nu_{\theta x}}, \quad (6b)$$

$$c_{66} = hG_{x\theta}; \quad c_{55} = hG_{xz}; \quad c_{44} = hG_{\theta z}; \quad D_{ij} = \frac{h^2}{12} c_{ij}. \quad (6c)$$

As far as the shear correction factors, results will be presented for the usual values of $k_1^2 = k_2^2 = \frac{5}{6}$. A discussion of various methods for determining these factors can be found in Dong and Nelson (1972) and Whitney (1973).

We shall use s_{ij} to denote the generalized stresses corresponding to the generalized linear strains, i.e., $s = C.e$. Using the asymptotic expansions for the strains gives the stresses as

$$\sigma_{ij} = \eta s_0 + \xi s_{ij}^{(1)} + \xi^2 \sigma_{ij}^{(2)} + \xi^3 \sigma_{ij}^{(3)} + \ldots. \quad (7a)$$

Notice that

$$\sigma_{ij}^0 = s_{ij}^0; \quad \sigma_{ij}^{(1)} = s_{ij}^{(1)}. \quad (7b)$$

$$N_x^{(2)} = c_{11} u_{,x}^{(2)} + c_{12} \frac{v_{,\theta}^{(2)} + w^{(2)}}{R} + c_{11} L_x(\mathbf{V}_1) + c_{12} L_\theta(\mathbf{V}_1), \quad (7c)$$

or, in abbreviated form,

$$\sigma^{(2)} = s^{(2)} + C.L(\mathbf{V}_1). \quad (7d)$$

The third-order generalized stresses can also be found in a similar fashion.

The relationship $\eta(\xi)$. In this subsection, we shall use the abbreviation $\frac{1}{2}\sigma\epsilon$ to denote the strain energy of the shell, which can be written in the form of an integral over the volume, V:

$$\frac{1}{2}\sigma\epsilon = \frac{1}{2}\int_0^l \int_0^{2\pi} (N_x\epsilon_x + N_\theta\epsilon_\theta + N_{x\theta}\gamma_{x\theta} + Q_{xz}\gamma_{xz} + Q_{\theta z}\gamma_{\theta z} + M_x\kappa_x + M_\theta\kappa_\theta + M_{x\theta}\kappa_{x\theta}) R d\theta dx. \quad (8a)$$

Also, we shall denote by Ω the work done by the uniform fluid pressure (which remains always normal to the surface as the shell deforms); this is the product of the pressure and the change in the volume enclosed by the shell. An expression in terms of the displacements can be found in Brush and Almroth (1975):

$$\Omega = p\int_0^l \int_0^{2\pi} \left[w + \frac{1}{2R}(v^2 - vw_{,\theta} + v_{,\theta}w + w^2) \right] R d\theta dx. \quad (8b)$$

A complete and extensive presentation of the $\eta(\xi)$ relationship is given in Budiansky (1974), in which use is made of Frechet derivatives. The formal definition given for Frechet derivatives of any order is entirely equivalent to the familiar process of "taking variations" in the calculus of variations. We shall use prime to denote Frechet derivatives and the subscript c means evaluation at the critical state.

If we set now

$$\eta = 1 + a\xi + b\xi^2, \quad (9a)$$

we can find the coefficients a, b for the case of linear stress-strain relations, quadratic strain-displacement relations, and quadratic shortening-displacement relations, as follows (Budiansky, 1974):

$$a = -\frac{3}{2}\frac{\sigma^{(1)}(\epsilon_c'' V_1^2)}{\sigma_c^0(\epsilon_c'' V_1^2) - (\Omega_c'' V_1^2)}, \quad (9b)$$

$$b = -\frac{2\sigma^{(1)}(\epsilon_c'' V_1 V_2) + \sigma^{(2)}(\epsilon_c'' V_1^2)}{\sigma_c^0(\epsilon_c'' V_1^2) - (\Omega_c'' V_1^2)}. \quad (9c)$$

Notice that the second term in the denominator is due to the hydrostatic loading and it would not exist in a dead-loading situation. Also, the variable V is identified as the set of functions u, v, w. The Frechet derivatives of the generalized strains are found to be

$$\epsilon_x'' V_1 V_2 = w_{,x}^{(1)} w_{,x}^{(2)}; \quad \epsilon_x'' V_1^2 = w_{,x}^{(1)2}, \quad (10a)$$

$$\epsilon_\theta'' V_1 V_2 = w_{,\theta}^{(1)} w_{,\theta}^{(2)}/R^2; \quad \epsilon_\theta'' V_1^2 = w_{,\theta}^{(1)2}, \quad (10b)$$

$$\gamma_{x\theta}'' V_1 V_2 = \frac{1}{R}(w_{,x}^{(1)} w_{,\theta}^{(2)} + w_{,x}^{(2)} w_{,\theta}^{(1)}); \quad \gamma_{x\theta}'' V_1^2 = 2w_{,x}^{(1)} w_{,\theta}^{(1)}/R. \quad (10c)$$

All the other components of the generalized strain result in zero Frechet second derivatives.

$$= p_c \iint (v^{(1)2} - v^{(1)} w^{(1)}_{,\theta\theta} + v^{(1)}_{,\theta} w^{(1)} + w^{(1)2}) d\theta dx. \quad (10d)$$

It is also to be noted that the derivation of the relationship $\eta(\xi)$ makes use of the orthogonality conditions

$$s^{(2)} e^{(1)} = s^{(1)} e^{(2)} = s^0 (\epsilon_c'' V_1 V_2) = 0. \quad (10e)$$

The First-Order Displacement Field

The governing equations of equilibrium and boundary conditions for the shear deformable orthotropic shell can be derived from the principle of virtual work, namely $\delta I = \delta\Omega$, by integrating by parts and setting the coefficients of δu, δv, δw, $\delta\phi$, and $\delta\psi$ to zero separately. Thus, one obtains

$$RN_{x,x} + N_{x\theta,\theta} = 0, \quad (11a)$$

$$RN_{x\theta,x} + N_{\theta,\theta} - p(v - w_{,\theta}) = 0, \quad (11b)$$

$$RM_{x,x} + M_{x\theta,\theta} - RQ_{xz} = 0, \quad (11c)$$

$$RM_{x\theta,x} + M_{\theta,\theta} - RQ_{\theta z} = 0, \quad (11d)$$

$$RQ_{xz,x} + Q_{\theta z,\theta} - N_\theta + R(N_x w_{,x})_{,x} + \frac{1}{R}(N_\theta w_{,\theta})_{,\theta}$$

$$+ (N_{x\theta} w_{,\theta})_{,x} + (N_{x\theta} w_{,x})_{,\theta} - p(v_{,\theta} + w) - pR = 0. \quad (11e)$$

Denoting prescribed quantities by *, the boundary conditions at $x = 0, l$ for the general case of a shell in which the end loading N_x^* or M_x^* may be nonzero, are

Either	Or
$u = u^*$	$N_x = N_x^*$
$v = v^*$	$N_{x\theta} = 0$
$w = w^*$	$N_x w_{,x} + N_{x\theta} \frac{w_{,\theta}}{R} + Q_{xz} = 0$
$\psi = \psi^*$	$M_x = M_x^*$
$\phi = \phi^*$	$M_{x\theta} = 0.$

We shall consider in the present paper a shell loaded by external pressure in a simply supported configuration and in which there are no prescribed end forces or moments. The boundary conditions in this case are simply

$$v = w = \phi = 0; \quad N_x = M_x = 0; \quad \text{at } x = 0, l. \quad (11f)$$

In the prebuckling state, the axially symmetric distribution of external forces produces stresses identical at all cross sections. For external pressure,

$$N_{\theta 0} = -pR; \quad N_{x0} = -\alpha pR/2; \quad N_{x\theta 0} = 0. \quad (12a)$$

The parameter α is used to conveniently allow for end pressure loading; if the pressure contributes to axial stress through end plates, $\alpha = 1$, whereas if the pressure only acts laterally, $\alpha = 0$. We shall also use the superscript c to refer to the critical state, i.e., $N_{\theta 0}^c = -p_c R$.

Substituting the asymptotic expansions (3) into the equilibrium Eqs. (11), retaining the first-order terms and then using the constitutive relations (6) to express the first-order resultant forces and moments in terms of the first-order displacements

$$Rc_{11} u^{(1)}_{,xx} + \frac{c_{66}}{R} u^{(1)}_{,\theta\theta} + (c_{12} + c_{66}) v^{(1)}_{,x\theta} + c_{12} w^{(1)}_{,x} = 0, \quad (13a)$$

$$(c_{12} + c_{66}) u^{(1)}_{,x\theta} + Rc_{66} v^{(1)}_{,xx} + \frac{c_{22}}{R} v^{(1)}_{,\theta\theta} - p_c v^{(1)}$$

$$+ \left(\frac{c_{22}}{R} + p_c\right) w^{(1)}_{,\theta} = 0, \quad (13b)$$

$$RD_{11} \psi^{(1)}_{,xx} + D_{66} \frac{\psi^{(1)}_{,\theta\theta}}{R} + (D_{12} + D_{66}) \phi^{(1)}_{,x\theta}$$

$$- Rk_1^2 c_{55} (\psi^{(1)} + w^{(1)}_{,x}) = 0, \quad (13c)$$

$$RD_{66} \phi^{(1)}_{,xx} + D_{22} \frac{\phi^{(1)}_{,\theta\theta}}{R} + (D_{12} + D_{66}) \psi^{(1)}_{,x\theta}$$

$$- k_2^2 c_{44} (R\phi^{(1)} + w^{(1)}_{,\theta}) = 0, \quad (13d)$$

$$-c_{12} u^{(1)}_{,x} - \left(\frac{c_{22}}{R} + p_c\right)(v^{(1)}_{,\theta} + w^{(1)}) + R(N_{x0}^c + k_1^2 c_{55}) w^{(1)}_{,xx}$$

$$+ (N_{\theta 0}^c + k_2^2 c_{44}) \frac{w^{(1)}_{,\theta\theta}}{R} + Rk_1^2 c_{55} \psi^{(1)}_{,x} + k_2^2 c_{44} \phi^{(1)}_{,\theta} = 0, \quad (13e)$$

and the first-order boundary conditions are

$$v^{(1)} = w^{(1)} = \phi^{(1)} = 0 \quad \text{at} \quad x = 0, l. \quad (13f)$$

$$c_{11} u^{(1)}_{,x} + \frac{c_{12}}{R}(v^{(1)}_{,\theta} + w^{(1)}) = 0;$$

$$D_{11} \psi^{(1)}_{,x} + \frac{D_{12}}{R} \phi^{(1)}_{,\theta} = 0 \quad \text{at} \quad x = 0, l \quad (13g)$$

The first-order displacement field is set in the form

$$u^{(1)}(x, \theta) = U_1 \sin n\theta \cos \lambda x;$$

$$v^{(1)}(x, \theta) = V_1 \cos n\theta \sin \lambda x, \quad (14a)$$

$$w^{(1)}(x, \theta) = W_1 \sin n\theta \sin \lambda x, \quad (14b)$$

$$\psi^{(1)}(x, \theta) = \Psi_1 \sin n\theta \cos \lambda x;$$

$$\phi^{(1)}(x, \theta) = \Phi_1 \cos n\theta \sin \lambda x. \quad (14c)$$

By setting

$$\lambda = \frac{m\pi}{l}, \quad (14c)$$

the boundary conditions (13f,g) are satisfied. Then, substituting into the differential equations (13a–e) gives a system of five linear algebraic homogeneous equations as follows:

$$\left(Rc_{11}\lambda^2 + \frac{c_{66}}{R} n^2\right) U_1 + (c_{12} + c_{66}) n\lambda V_1 - c_{12}\lambda W_1 = 0, \quad (15a)$$

$$(c_{12} + c_{66}) n\lambda U_1 + \left(Rc_{66}\lambda^2 + \frac{c_{22}}{R} n^2 + p_c\right) V_1$$

$$- \left(\frac{c_{22}}{R} + p_c\right) n W_1 = 0, \quad (15b)$$

$$Rk_1^2 c_{55}\lambda W_1 + \left(RD_{11}\lambda^2 + \frac{D_{66}}{R} n^2 + Rk_1^2 c_{55}\right) \Psi_1$$

$$+ (D_{12} + D_{66}) n\lambda \Phi_1 = 0, \quad (15c)$$

$$k_2^2 c_{44} n W_1 + (D_{12} + D_{66}) n \lambda \Psi_1 + \left(RD_{66}\lambda^2 + \frac{D_{22}}{R} n^2 + Rk_2^2 c_{44} \right) \Phi_1 = 0, \quad (15d)$$

$$c_{12}\lambda U_1 + \left(\frac{c_{22}}{R} + p_c \right) n V_1 - \left[\frac{c_{22}}{R} + R(N_{x0}^c + k_1^2 c_{55})\lambda^2 + (N_{\theta 0}^c + k_2^2 c_{44}) \frac{n^2}{R} + p_c \right] W_1 - Rk_1^2 c_{55}\lambda \Psi_1 - k_2^2 c_{44} n \Phi_1 = 0. \quad (15e)$$

Setting the five-by-five determinant to zero gives a quadratic equation; the minimum positive root is the critical pressure, p_c. The buckling modes, i.e., the constants U_1, V_1, W_1, Ψ_1, and Φ_1, are subsequently obtained by choosing the normalization $W_1 = h$, where h is the shell thickness.

Second-Order Displacements

Substituting the asymptotic expansions (3) into the equilibrium Eqs. (11), retaining the ξ^2 terms and using the anticipated result that $p = p_c + O(\xi^2)$, gives the second-order equilibrium equations as follows:

$$RN_{x,x}^{(2)} + N_{x\theta,\theta}^{(2)} = 0, \quad (16a)$$

$$RN_{x\theta,x}^{(2)} + N_{\theta,\theta}^{(2)} - p_c(v^{(2)} - w_{,\theta}^{(2)}) = 0, \quad (16b)$$

$$RM_{x,x}^{(2)} + M_{x\theta,\theta}^{(2)} - RQ_{xz}^{(2)} = 0, \quad (16c)$$

$$RM_{x\theta,x}^{(2)} + M_{\theta,\theta}^{(2)} - RQ_{\theta z}^{(2)} = 0, \quad (16d)$$

$$RQ_{xz,x}^{(2)} + Q_{\theta z,\theta}^{(2)} - N_\theta^{(2)} + R(N_{x0}^c w_{,x}^{(2)} + N_x^{(1)} w_{,x}^{(1)})_{,x} + \frac{1}{R}(N_{\theta 0}^c w_{,\theta}^{(2)} + N_\theta^{(1)} w_{,\theta}^{(1)})_{,\theta} + (N_{x\theta}^{(1)} w_{,x}^{(1)})_{,\theta} + (N_{x\theta}^{(1)} w_{,\theta}^{(1)})_{,x} - p_c(v_{,\theta}^{(2)} + w^{(2)}) = 0. \quad (16e)$$

Substituting the resultant force-displacement relations gives the following differential equations for the second-order displacement field:

$$Rc_{11}u_{,xx}^{(2)} + \frac{c_{66}}{R} u_{,\theta\theta}^{(2)} + (c_{12} + c_{66}) v_{,x\theta}^{(2)} + c_{12} w_{,x}^{(2)} + Rc_{11} w_{,x}^{(1)} w_{,xx}^{(1)} + \frac{c_{66}}{R} w_{,x}^{(1)} w_{,\theta\theta}^{(1)} + \frac{c_{12} + c_{66}}{R} w_{,\theta}^{(1)} w_{,x\theta}^{(1)} = 0, \quad (17a)$$

$$(c_{12} + c_{66}) u_{,x\theta}^{(2)} + Rc_{66} v_{,xx}^{(2)} + \frac{c_{22}}{R} v_{,\theta\theta}^{(2)} - p_c v^{(2)} + \left(\frac{c_{22}}{R} + p_c \right) w_{,\theta}^{(2)} + c_{66} w_{,\theta}^{(1)} w_{,xx}^{(1)} + (c_{12} + c_{66}) w_{,x}^{(1)} w_{,x\theta}^{(1)} + \frac{c_{22}}{R^2} w_{,\theta}^{(1)} w_{,\theta\theta}^{(1)} = 0, \quad (17b)$$

$$RD_{11}\psi_{,xx}^{(2)} + D_{66} \frac{\psi_{,\theta\theta}^{(2)}}{R} + (D_{12} + D_{66}) \phi_{,x\theta}^{(2)} - Rk_1^2 c_{55}(\psi^{(2)} + w_{,x}^{(2)}) = 0, \quad (17c)$$

$$RD_{66}\phi_{,xx}^{(2)} + D_{22} \frac{\phi_{,\theta\theta}^{(2)}}{R} + (D_{12} + D_{66}) \psi_{,x\theta}^{(2)} - k_2^2 c_{44}(R\phi^{(2)} + w_{,\theta}^{(2)}) = 0, \quad (17d)$$

$$-Rc_{12}u_{,x}^{(2)} - (c_{22} + p_c R)(v_{,\theta}^{(2)} + w^{(2)}) + R^2(N_{x0}^c + k_1^2 c_{55}) w_{,xx}^{(2)} + (N_{\theta 0}^c + k_2^2 c_{44}) w_{,\theta\theta}^{(2)} + R^2 k_1^2 c_{55} \psi_{,x}^{(2)} + Rk_2^2 c_{44} \phi_{,\theta}^{(2)} - \frac{Rc_{12}}{2} w_{,x}^{(1)2} - \frac{c_{22}}{2R} w_{,\theta}^{(1)2} + [Rc_{11}u_{,x}^{(1)} + c_{12}(v_{,\theta}^{(1)} + w^{(1)})] R w_{,xx}^{(1)} + [Rc_{11}u_{,xx}^{(1)} + c_{12}(v_{,x\theta}^{(1)} + w_{,x}^{(1)})] R w_{,x}^{(1)} + \left[c_{12}u_{,x}^{(1)} + \frac{c_{22}}{R}(v_{,\theta}^{(1)} + w^{(1)}) \right] w_{,\theta\theta}^{(1)} + \left[c_{12}u_{,x\theta}^{(1)} + \frac{c_{22}}{R}(v_{,\theta\theta}^{(1)} + w_{,\theta}^{(1)}) \right] w_{,\theta}^{(1)} + c_{66}R \left[2\left(v_{,x}^{(1)} + \frac{u_{,\theta}^{(1)}}{R} \right) w_{,x\theta}^{(1)} + \left(v_{,x\theta}^{(1)} + \frac{u_{,\theta\theta}^{(1)}}{R} \right) w_{,x}^{(1)} + \left(v_{,xx}^{(1)} + \frac{u_{,x\theta}^{(1)}}{R} \right) w_{,\theta}^{(1)} \right] = 0. \quad (17e)$$

Furthermore, the second-order boundary conditions are

$$v^{(2)} = w^{(2)} = \phi^{(2)} = 0 \quad \text{at} \quad x = 0, l. \quad (17f)$$

$$N_x^{(2)} = c_{11}u_{,x}^{(2)} + \frac{c_{12}}{R}(v_{,\theta}^{(2)} + w^{(2)}) + \frac{c_{11}}{2} w_{,x}^{(1)2} + \frac{c_{12}}{2R^2} w_{,\theta}^{(1)2} = 0 \quad (17g)$$

$$M_x^{(2)} = D_{11}\psi_{,x}^{(2)} + \frac{D_{12}}{R}\phi_{,\theta}^{(2)} = 0 \quad \text{at} \quad x = 0, l \quad (17h)$$

The quadratic terms involving the first-order displacements on the right-hand sides of the equations give rise to nonhomogeneous terms which are either independent of the θ coordinate or vary as $\cos 2n\theta$ or $\sin 2n\theta$. Thus, the second-order displacement is sought in the separated form:

$$u^{(2)}(x, \theta) = U_{20}(x) + U_{22}(x) \cos 2n\theta;$$
$$v^{(2)}(x, \theta) = V_{20}(x) + V_{22}(x) \sin 2n\theta, \quad (18a)$$
$$w^{(2)}(x, \theta) = W_{20}(x) + W_{22}(x) \cos 2n\theta;$$

$$\psi^{(2)}(x, \theta) = \Psi_{20}(x) + \Psi_{22}(x) \cos 2n\theta, \quad (18b)$$

$$\Phi^{(2)}(x, \theta) = \Phi_{20}(x) + \Phi_{22}(x) \sin 2n\theta. \quad (18c)$$

Notice that this second-order displacement field satisfies the orthogonality requirements (15a,b), namely, $s^{(2)}e^{(1)} = s^0(\epsilon_c'' V_1 V_2) = 0$, since

$$\int_0^{2\pi} \cos n\theta d\theta = \int_0^{2\pi} \sin n\theta d\theta = \int_0^{2\pi} \cos n\theta \cos 2n\theta d\theta = \int_0^{2\pi} \sin n\theta \cos 2n\theta d\theta = 0.$$

Substituting (18) into (17) gives in terms of

$$b_1 = R^2 \left[c_{11}U_1\lambda + \frac{c_{12}}{R}(V_1 n - W_1) \right] W_1 \lambda^2 + \left[c_{12}U_1\lambda + \frac{c_{22}}{R}(V_1 n - W_1) \right] W_1 n^2, \quad (19a)$$

$$b_2 = -R^2\left[c_{11}U_1\lambda + \frac{c_{12}}{R}\left(V_1 n - \frac{W_1}{2}\right)\right]W_1\lambda^2$$

$$- c_{66}R\left(V_1\lambda + \frac{U_1 n}{R}\right)W_1\lambda n, \quad (19b)$$

$$b_3 = -\left[c_{12}U_1\lambda + \frac{c_{22}}{R}\left(V_1 n - \frac{W_1}{2}\right)\right]W_1 n^2$$

$$- c_{66}R\left(V_1\lambda + \frac{U_1 n}{R}\right)W_1\lambda n, \quad (19c)$$

$$b_4 = 2c_{66}R\left(V_1\lambda + \frac{U_1 n}{R}\right)W_1\lambda n, \quad (19d)$$

two sets of ordinary differential equations, one set for the functions in the θ-independent terms of (18) and another set for the functions in the θ-dependent terms.

The first set consists of the following five ordinary differential equations for $U_{20}(x)$, $V_{20}(x)$, $W_{20}(x)$, $\Psi_{20}(x)$, and $\Phi_{20}(x)$:

$$Rc_{11}U''_{20}(x) + c_{12}W'_{20}(x) + [(c_{12} + c_{66})n^2$$

$$- R^2c_{11}\lambda^2 - c_{66}n^2]\frac{W_1^2}{4R}\lambda \sin 2\lambda x = 0, \quad (20a)$$

$$Rc_{66}V''_{20}(x) - p_cV_{20}(x) = 0, \quad (20b)$$

$$D_{11}\Psi''_{20}(x) - k_1^2c_{55}[\Psi_{20}(x) + W'_{20}(x)] = 0, \quad (20c)$$

$$D_{66}\Phi''_{20}(x) - k_2^2c_{44}\Phi_{20}(x) = 0, \quad (20d)$$

$$R^2(k_1^2c_{55} + N^c_{x0})W''_{20}(x) - (c_{22} + p_cR)W_{20}(x)$$

$$- Rc_{12}U'_{20}(x) + R^2k_1^2c_{55}\Psi'_{20}(x)$$

$$+ \tfrac{1}{2}[(b_1 + b_3)\sin^2\lambda x + (b_2 + b_4)\cos^2\lambda x] = 0. \quad (20e)$$

Also, the corresponding boundary conditions (17) give at the ends of the shell:

$$V_{20} = W_{20} = \Phi_{20} = 0; \quad \text{at} \quad x = 0, l, \quad (20f)$$

and

$$\Psi'_{20} = 0; \quad c_{11}U'_{20} = -c_{11}\lambda^2\frac{W_1^2}{4}; \quad \text{at} \quad x = 0, l. \quad (20g)$$

Likewise, the second set consists of the following five ordinary differential equations for $U_{22}(x)$, $V_{22}(x)$, $W_{22}(x)$, $\Psi_{22}(x)$, and $\Phi_{22}(x)$:

$$Rc_{11}U''_{22}(x) - \frac{c_{66}}{R}4n^2U_{22}(x) + (c_{12} + c_{66})2nV'_{22}(x)$$

$$+ c_{12}W'_{22}(x) + [(c_{12} + c_{66})n^2 + R^2c_{11}\lambda^2 + c_{66}n^2]$$

$$\times \frac{W_1^2}{4R}\lambda \sin 2\lambda x = 0, \quad (21a)$$

$$Rc_{66}V''_{22}(x) - \left(\frac{c_{22}}{R}4n^2 + p_c\right)V_{22}(x) - (c_{12} + c_{66})2nU'_{22}(x)$$

$$- \left(\frac{c_{22}}{R} + p_c\right)2nW_{22}(x) + \left[(c_{12} + c_{66})\lambda^2\cos^2\lambda x\right.$$

$$\left. - c_{66}\lambda^2\sin^2\lambda x - \frac{c_{22}}{R^2}n^2\sin^2\lambda x\right]\frac{W_1^2}{2}n = 0, \quad (21b)$$

$$RD_{11}\Psi''_{22}(x) - \left(\frac{D_{66}}{R}4n^2 + Rk_1^2c_{55}\right)\Psi_{22}(x)$$

$$+ (D_{12} + D_{66})2n\Phi'_{22}(x) - Rk_1^2c_{55}W'_{22}(x) = 0, \quad (21c)$$

$$RD_{66}\Phi''_{22}(x) - \left(\frac{D_{22}}{R}4n^2 + Rk_2^2c_{44}\right)\Phi_{22}(x)$$

$$- (D_{12} + D_{66})2n\Psi'_{22}(x) + k_2^4c_{44}2nW_{22}(x) = 0, \quad (21d)$$

$$R^2(k_1^2c_{55} + N^c_{x0})W''_{22}(x)$$

$$- [(k_2^2c_{44} + N^c_{\theta 0})4n^2 + c_{22} + p_cR]W_{22}(x)$$

$$- Rc_{12}U'_{22}(x) - (c_{22} + p_cR)2nV_{22}(x)$$

$$+ R^2k_1^2c_{55}\Psi'_{22}(x) + Rk_2^2c_{44}2n\Phi_{22}(x)$$

$$+ \tfrac{1}{2}[(b_3 - b_1)\sin^2\lambda x + (b_4 - b_2)\cos^2\lambda x] = 0. \quad (21e)$$

Also, the conditions at the ends are

$$V_{22} = W_{22} = \Phi_{22} = 0; \quad \text{at} \quad x = 0, l, \quad (21f)$$

and

$$\Psi'_{22} = 0; \quad c_{11}U'_{22} = c_{11}\lambda^2\frac{W_1^2}{4}; \quad \text{at} \quad x = 0, l. \quad (21g)$$

However, due to symmetry only half of the shell need be considered in the solution procedure. Indeed, the symmetry of the shell deformation imposes for $0 \le x \le l/2$:

$$U(l - x) = -U(x); \quad V(l - x) = V(x);$$

$$W(l - x) = W(x), \quad (22a)$$

$$\Psi(l - x) = -\Psi(x); \quad \Phi(l - x) = \Phi(x). \quad (22b)$$

Therefore, at the midpoint of the shell, i.e., at $x = l/2$, $u = v' = w' = \psi = \phi' = 0$ allows solving for half the shell length and replacing the conditions (20f,g) at $x = l$ with

$$U_{20} = V'_{20} = W'_{20} = \Psi_{20} = \Phi'_{20} = 0 \quad \text{at} \quad x = l/2 \quad (22c)$$

and also allows replacing the conditions (21f, g) at $x = l$, with

$$U_{22} = V'_{22} = W'_{22} = \Psi_{22} = \Phi'_{22} = 0 \quad \text{at} \quad x = l/2. \quad (22d)$$

Solution Details. The two-point boundary value problem for half of the shell is solved separately for the θ-independent and the θ-dependent functions by the relaxation method (Press et al, 1989), in which the five coupled ordinary differential equations are replaced by finite difference equations on a mesh of points that spans half the length of the shell. The method produces a matrix equation to be solved, but the matrix takes a special, "block diagonal" form, that allows it to be inverted far more efficiently both in time and storage than would be possible for a general matrix.

In the implementation of the method for the functions of the θ-independent term of (18), ten functions of x are defined as follows: $y_1 = V_{20}$, $y_2 = W_{20}$, $y_3 = \Psi'_{20}$, $y_4 = U'_{20}$, $y_5 = \Phi_{20}$, $y_6 = U_{20}$, $y_7 = V'_{20}$, $y_8 = W'_{20}$, $y_9 = \Psi_{20}$, and $y_{10} = \Phi'_{20}$. The ten first-order coupled ordinary differential equations for the ten y's are $y'_1 = y_7$, Eq. (20a), $y'_2 = y_8$, Eq. (20b), $y'_9 = y_3$, Eq. (20c), $y'_6 = y_4$, Eq. (20d), $y'_5 = y_{10}$, and Eq. (20e). The corresponding ten boundary conditions are Eqs. (20f,g) at $x = 0$ and (22c) at $x = l/2$.

It should be noted that in order to exploit the reduced storage allowed by operating on blocks, the functions should be defined in such order so as pivot elements can be found among the first five rows of the matrix. This means that the five boundary conditions at the first point must contain some dependence on the first five dependent variables y_1, y_2, y_3, y_4, and y_5. An

examination of the boundary conditions (20f,g) shows that defining the y_i's as outlined would satisfy this requirement. Regarding other details of the method, an equally spaced mesh of 241 points was employed and the procedure turned out to be highly efficient with rapid convergence. As an initial guess for the iteration process, the closed-form solution for a very long cylinder (as outlined below) was used for the displacements. An investigation of the convergence showed that essentially the same results were produced with even three times as many mesh points.

In a similar fashion, the procedure involves solving a separate two-point boundary value problem for the U_{22}, V_{22}, etc., i.e., by defining $y_1 = V_{22}$, $y_2 = W_{22}$, $y_3 = \Psi'_{22}$, $y_4 = U'_{22}$, $y_5 = \Phi_{22}$, $y_6 = U_{22}$, $y_7 = V'_{22}$, $y_8 = W'_{22}$, $y_9 = \Psi_{22}$, and $y_{10} = \Phi'_{22}$ and using the differential equations (21a–e) together with the boundary conditions (21f,g) and (22d).

Initial Post-buckling Variation of Pressure

Once the second-order displacement field is determined from the solution of the foregoing two-point boundary value problem, the post-buckling coefficient, b, can be determined from (9) and (10).

Notice first that the coefficient $a = 0$, as expected, since

$$\sigma^{(1)}(\epsilon_c'' V_1^2) = \int_0^{2\pi}\int_0^{l}\left(N_x^{(1)} w_{,x}^{(1)2} + N_\theta^{(1)}\frac{w_{,\theta}^{(1)2}}{R^2} + 2N_{x\theta}^{(1)}\frac{w_{,x}^{(1)} w_{,\theta}^{(1)}}{R}\right)dxd\theta. \quad (23a)$$

Substituting the first-order resultant forces and moments in terms of the first-order displacement field by using (6a) and integrating with respect to θ involves the integrals

$$\int_0^{2\pi}\cos n\theta \sin^2 n\theta d\theta = \int_0^{2\pi}\cos^3 n\theta d\theta = \int_0^{2\pi}\sin n\theta \sin 2n\theta d\theta = 0. \quad (23b)$$

Therefore,

$$\sigma^{(1)}(\epsilon_c'' V_1^2) = 0. \quad (23c)$$

This verifies that the initial variation of pressure after buckling is

$$\eta = p/p_c = 1 + b(\delta/h)^2, \quad (24)$$

where, since the buckling modes were normalized so that W_1 is equal to the shell thickness, h, the general perturbation variable ξ has been replaced by δ/h, the maximum amplitude of the buckling mode over the shell thickness.

Returning to the post-buckling coefficient, b, the denominator term in (9c) is

$$\sigma_c^0(\epsilon_c'' V_1^2) = -\int_0^{2\pi}\int_0^{l}\left(N_{x0}^c w_{,x}^{(1)2} + N_{\theta 0}^c\frac{w_{,\theta}^{(1)2}}{R^2} + 2N_{x\theta 0}^c\frac{w_{,x}^{(1)} w_{,\theta}^{(1)}}{R}\right)dxd\theta. \quad (25a)$$

Substituting the first-order displacement field (14) and integrating with respect to θ gives

$$\sigma_c^0(\epsilon_c'' V_1^2) = -\left(N_{x0}^c\lambda^2 + N_{\theta 0}^c\frac{n^2}{R^2}\right)W_1^2\frac{\pi L}{2}dx. \quad (25b)$$

The first term in the numerator in (9c) becomes

$$\sigma^{(1)}(\epsilon_c'' V_1 V_2) = \int_0^{2\pi}\int_0^{l}\left[N_x^{(1)} w_{,x}^{(1)} w_{,x}^{(2)} + N_\theta^{(1)}\frac{w_{,\theta}^{(1)} w_{,\theta}^{(2)}}{R^2} + \frac{N_{x\theta}^{(1)}}{R}(w_{,x}^{(1)} w_{,\theta}^{(2)} + w_{,x}^{(2)} w_{,\theta}^{(1)})\right]dxd\theta. \quad (26a)$$

Substituting the first-order resultant forces in terms of the first-order displacement fields by use of (6a) and (1) and integrating with respect to θ gives

$$\sigma^{(1)}(\epsilon_c'' V_1 V_2) = \int_0^{l}\left[f_1(x)\frac{\sin 2\lambda x}{2} - W_{22}(x)n(b_2 n \sin^2\lambda x + b_3\lambda\cos^2\lambda x)\right]W_1\pi dx, \quad (26b)$$

where

$$f_1(x) = W'_{20}(x)(b_1\lambda + b_3 n) + W'_{22}(x)\frac{b_3 n - b_1\lambda}{2}. \quad (26c)$$

Finally, the second term in the numerator in (9c) is

$$\sigma^{(2)}(\epsilon_c'' V_1^2) = \int_0^{2\pi}\int_0^{l}\left(N_x^{(2)} w_{,x}^{(1)2} + N_\theta^{(2)}\frac{w_{,\theta}^{(1)2}}{R^2} + 2N_{x\theta}^{(2)}\frac{w_{,x}^{(1)} w_{,\theta}^{(1)}}{R}\right)dxd\theta. \quad (27a)$$

Substituting the first and second-order resultant forces and moments in terms of the first and second-order displacement fields by using (6a) and (4) and integrating with respect to θ gives

$$\sigma^{(2)}(\epsilon_c'' V_1^2) = \int_0^{l}\left[f_2(x)\lambda^2\cos^2\lambda x + f_3(x)\frac{n^2}{R^2}\sin^2\lambda x + f_4(x)\frac{n\lambda}{R}\sin 2\lambda x\right]\pi\frac{W_1^2}{2}dx, \quad (27b)$$

where

$$f_2(x) = c_{11}[2U'_{20}(x) - U'_{22}(x)] + \frac{c_{12}}{R}[2W_{20}(x) - 2nV_{22}(x) - W_{22}(x)] + \frac{c_{11}}{4}W_1^2\lambda^2\cos^2\lambda x + \frac{c_{12}}{4R^2}W_1^2 n^2\sin^2\lambda x, \quad (27c)$$

$$f_3(x) = c_{12}[2U'_{20}(x) - U'_{22}(x)] + \frac{c_{22}}{R}[2W_{20}(x) - 2nV_{22}(x) - W_{22}(x)] + \frac{c_{12}}{4}W_1^2\lambda^2\cos^2\lambda x + \frac{c_{22}}{4R^2}W_1^2 n^2\sin^2\lambda x, \quad (27d)$$

and

$$f_4(x) = c_{66}\left[V'_{22}(x) - U_{22}(x)\frac{2n}{R}\right] + \frac{c_{66}}{4R}W_1^2 n\lambda\sin 2\lambda x. \quad (27e)$$

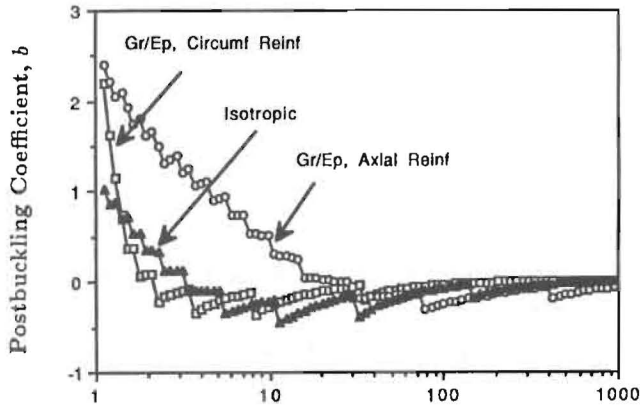

$$\tilde{z} = \frac{\ell^2\left(c_{11}c_{22}-c_{12}^2\right)^{1/2}}{R\sqrt{12}(c_{11}c_{22}D_{11}D_{22})^{1/4}}$$

Fig. 1 Post-buckling coefficient, b, calculated from the shear deformable theory, for the cases of circumferentially reinforced, axially reinforced graphite/epoxy, and isotropic material, in a shell under lateral external pressure only

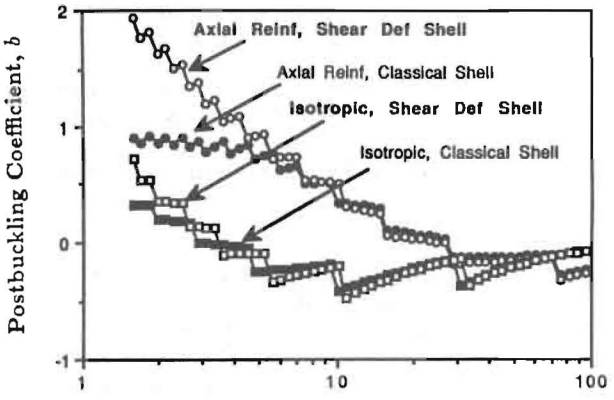

$$\tilde{z} = \frac{\ell^2\left(c_{11}c_{22}-c_{12}^2\right)^{1/2}}{R\sqrt{12}(c_{11}c_{22}D_{11}D_{22})^{1/4}}$$

Fig. 3 The effect of transverse shear on the postbuckling coefficient, b, for lateral external pressure loading

One additional term is from the effect of the external pressure

$$\Omega'' V_1^2 = p\int_0^{2\pi}\int_0^{l}(v^{(1)2} - v^{(1)}w_{,\theta}^{(1)} + v_{,\theta}^{(1)}w^{(1)} + w^{(1)2})\,d\theta dx. \tag{27e}$$

Substituting the first-order displacement field and integrating gives

$$\Omega'' V_1^2 = p(V_1^2 - 2V_1W_1n + W_1^2)\frac{\pi L}{2}. \tag{27e}$$

A standard method of numerical integration is used to calculate the post-buckling coefficient b from these expressions. The character of the post-buckling behavior in the initial stages after buckling hinges on the sign and magnitude of b. If b is positive, the applied load (external pressure) increases to values above the critical load p_c with increasing buckling deflection. However, if b turns out to be negative, then the equilibrium load falls with increasing buckling deflection and the post-buckling behavior is unstable.

Results and Discussion

Let us consider a shell being made of unidirectional graphite/epoxy with the following typical properties for the material (1 is along the fibers, 2 is the in-plane transverse, and 3 is the out-of-plane transverse direction): moduli in GN/m^2 $E_1 = 140.0$, $E_2 = 9.1$, $G_{12} = G_{23} = G_{31} = 4.3$, and Poisson's ratio $\nu_{12} = 0.300$. The shear correction factors are assumed to be $k_1^2 = k_2^2 = \frac{5}{6}$. The shell has a mean radius of $R = 1$ m. Two cases of shell thickness are considered in the following, one corresponding to radii ratio $R_2/R_1 = 1.05$ and another thicker construction with $R_2/R_1 = 1.10$. Also, two cases of loading are considered: lateral only external pressure loading, i.e., no axial load and $\alpha = 0$ in (12a), and external pressure with hydrostatic end loading, i.e., with axial compressive loads determined from (12a) with $\alpha = 1$.

The Batdorf parameter has been used as a convenient nondimensional parameter to present results for shell buckling and post-buckling. For isotropic cylindrical shells, this is only a function of the geometry and is defined as $\bar{z} = l^2/Rh$ where l is the length, R is the mean radius, and h the thickness of the shell. Analogues for anisotropy have been derived by Nemeth (1994) by performing a nondimensionalization of the shell buckling equations and it was shown that, for anisotropic shells, the Batdorf parameter depends not only on the geometry but

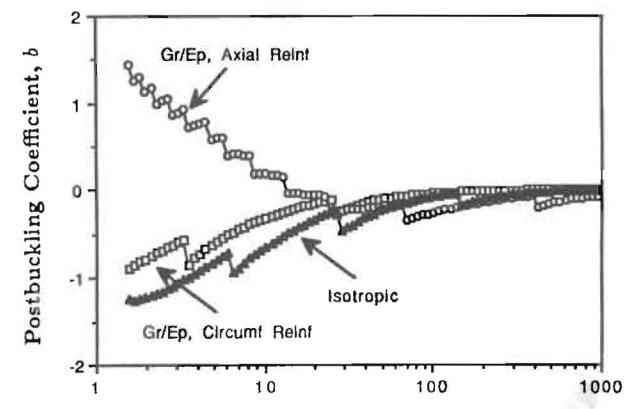

$$\tilde{z} = \frac{\ell^2\left(c_{11}c_{22}-c_{12}^2\right)^{1/2}}{R\sqrt{12}(c_{11}c_{22}D_{11}D_{22})^{1/4}}$$

Fig. 2 Post-buckling coefficient, b, from the shear deformable shell theory for the case of hydrostatic end loading

Table 1 Effect of the anisotropy Post-buckling coefficient, b

Lateral External Pressure Only, $R = 1$m, $R_2/R_1 = 1.10$, $k_1^2 = k_2^2 = 5/6$

$\bar{z}$*	b Circumf† Reinf	b Axial‡ Reinf	b Isotropic**
2	0.0847	1.6421	0.3483
5	−0.2170	0.9241	−0.0949
10	−0.2681	0.5118	−0.2075
23	−0.0839	0.0152	−0.2052
53	−0.0934	−0.1460	−0.1940
120	−0.0232	−0.2119	−0.0474
271	0.0001	−0.0916	−0.0618
615	0.0064	−0.1102	−0.0101
1,395	0.0078	−0.0339	0.0043
3,162	0.0081	−0.0036	0.0075

* Batdorf Parameter for orthotropy, $\bar{z} = l^2(c_{11}c_{22} - c_{12}^2)^{1/2}/[R\sqrt{12}(c_{11}c_{22}D_{11}D_{22})^{1/4}]$.
† Gr/Ep, Circumferential Reinforcement, moduli in GN/m^2: $E_x = 9.1$, $E_\theta = 140.0$, $G_{x\theta} = G_{\theta z} = G_{xz} = 4.3$, and Poisson's ratio $\nu_{x\theta} = 0.020$.
‡ Gr/Ep, Axial Reinforcement, moduli in GN/m^2: $E_x = 140.0$, $E_\theta = 9.1$, $G_{x\theta} = G_{\theta z} = G_{xz} = 4.3$, and Poisson's ratio $\nu_{x\theta} = 0.300$.
** For Isotropic, $E = 140.0$ GN/m^2, and $\nu = 0.300$.

Table 2 Effect of hydrostatic end loading post-buckling coefficient, b

R = 1m, R_2/R_1 = 1.10, $k_1^2 = k_2^2$ = 5/6

$\bar{z}$*	b	b	b	b
	Circumf Reinf†		Axial reinf‡	
	Lateral only	w/End pressure	Lateral only	w/End pressure
2	0.0847	−0.7760	1.6421	1.1391
5	−0.2170	−0.6034	0.9241	0.5963
10	−0.2681	−0.3189	0.5118	0.1941
23	−0.0839	−0.1283	0.0152	−0.0664
53	−0.0934	−0.0975	−0.1460	−0.1767
120	−0.0232	−0.0286	−0.2119	−0.2207
271	0.0001	−0.0035	−0.0916	−0.0968
615	0.0064	0.0039	−0.1102	−0.1111
1,395	0.0078	0.0059	−0.0339	−0.0353
3,162	0.0081	0.0006	−0.0036	−0.0050

* Batdorf Parameter for orthotropy, $\bar{z} = l^2(c_{11}c_{22} - c_{12}^2)^{1/2}/[R\sqrt{12}(c_{11}c_{22}D_{11}D_{22})^{1/4}]$.
† Gr/Ep, Circumferential Reinforcement, moduli in GN/m^2: E_x = 9.1, E_θ = 140.0, $G_{x\theta} = G_{\theta z} = G_{xz}$ = 4.3, and Poisson's ratio $\nu_{x\theta}$ = 0.020.
‡ Gr/Ep, Axial Reinforcement, moduli in GN/m^2: E_x = 140.0, E_θ = 9.1, $G_{x\theta} = G_{\theta z} = G_{xz}$ = 4.3, and Poisson's ratio $\nu_{x\theta}$ = 0.300.

also on the stiffness constants. In particular, for an orthotropic cylindrical shell, the Batdorf parameter becomes

$$\bar{z} = \frac{l^2(c_{11}c_{22} - c_{12}^2)^{1/2}}{R\sqrt{12}(c_{11}c_{22}D_{11}D_{22})^{1/4}}, \tag{28}$$

where c_{ij} and D_{ij} are defined in (6b, c).

The post-buckling coefficient b is calculated following the solution of the two-point boundary value problem for the second-order displacements, as has already been outlined. If b is negative, the shell is imperfection-sensitive and the load carrying capacity diminishes following buckling. Also, the degree of imperfection-sensitivity is governed by the magnitude of b. If, on the other hand, b is positive, the structure retains some ability to support increased loads once bifurcation has taken place.

In all cases considered the structure buckles at m = 1, whereas n depends on the shell length, l, becoming equal to 2 for very long shells. The transition from one value of n to the next lower causes an abrupt change in b which explains the lack of smoothness of the b versus l curves in Figs. 1, 2, and 3. Budiansky and Amazigo (1968), in their isotropic classical shell solution, defined $\zeta = n^2l^2/\pi^2R^2$ and found the critical load by making the simplifying assumption that ζ may vary continuously and executing a formal minimization of the pressure function of ζ; this led to smooth b versus l curves.

Table 1 and Fig. 1 give b, calculated from the shear deformable theory, for the cases of circumferentially reinforced, axially reinforced graphite/epoxy, and isotropic material in a shell under lateral external pressure only, and for radii ratio, R_2/R_1 = 1.10. The main conclusion is that the regions of imperfection sensitivity are strongly dependent on the anisotropy of the material. For the circumferentially reinforced case, it can be concluded that the critical pressure (at the bifurcation point) ought to be reliable above $\bar{z} \simeq 270$, whereas for the axially reinforced case the structure is imperfection-

Table 3 Effect of the transverse shear post-buckling coefficient, b

Graphite/Epoxy, Circumferential Reinforcement, moduli GN/m^2: E_x = 9.1, E_θ = 140.0, $G_{x\theta} = G_{\theta z} = G_{xz}$ = 4.3, and Poisson's ratio $\nu_{x\theta}$ = 0.020
Lateral External Pressure Only, R = 1m, R_2/R_1 = 1.10, $k_1^2 = k_2^2$ = 5/6

$\bar{z}$*	b	b
	Shear Def Shell	Classical Shell
8	0.874	−0.3852	−0.1918
10	0.977	−0.2681	−0.1598
16	1.236	−0.1418	−0.0990
23	1.482	−0.0839	−0.0604
53	2.250	−0.0934	−0.0748
120	3.386	−0.0232	−0.0196
222	4.605	−0.0033	−0.0020
271	5.088	0.0001	0.0010
615	7.664	0.0064	0.0067
1,395	11.543	0.0078	0.0080
3,162	17.379	0.0081	0.0082

* Batdorf Parameter for orthotropy, $\bar{z} = l^2(c_{11}c_{22} - c_{12}^2)^{1/2}/[R\sqrt{12}(c_{11}c_{22}D_{11}D_{22})^{1/4}]$.

Table 4 Effect of thickness post-buckling coefficient, b

Lateral External Pressure Only, R = 1m, $k_1^2 = k_2^2$ = 5/6

l/R	b (n)	b (n)	b (n)	b (n)
	Circumf Reinf†		Axial Reinf‡	
	R_2/R_1 = 1.05	R_2/R_1 = 1.10	R_2/R_1 = 1.05	R_2/R_1 = 1.10
0.4	−0.1680 (6)	0.3775 (7)	0.9958 (15*)	1.7581 (15*)
0.5	−0.2319 (5*)	−0.1457 (5*)	0.7619 (12*)	1.3482 (12*)
0.7	−0.2347 (4*)	−0.2095 (4*)	0.3978 (9*)	0.9284 (9*)
1.0	−0.1011 (4)	−0.2511 (3)	0.0358 (7)	0.3097 (6)
2.0	−0.0328 (3)	−0.1373 (2)	−0.1616 (5)	−0.1627 (4)
4.0	−0.0133 (2*)	−0.0102 (2*)	−0.0833 (4)	−0.1570 (3)
5.0	−0.0054 (2*)	−0.0004 (2*)	−0.1045 (3*)	−0.0958 (3*)
6.0	−0.0019 (2*)	0.0037 (2*)	−0.0662 (3*)	−0.0566 (3*)
8.0	0.0007 (2*)	0.0067 (2*)	−0.0284 (3)	−0.0985 (2)
10.0	0.0015 (2*)	0.0075 (2*)	−0.0121 (3)	−0.0535 (2)

* Denotes buckling at the same same (n, m) for both R_2/R_1 ratios of 1.05 and 1.10.
† Gr/Ep, Circumferential Reinforcement, moduli in GN/m^2: E_x = 9.1, E_θ = 140.0, $G_{x\theta} = G_{\theta z} = G_{xz}$ = 4.3, and Poisson's ratio $\nu_{x\theta}$ = 0.020.
‡ Gr/Ep, Axial Reinforcement, moduli in GN/m^2: E_x = 140.0, E_θ = 9.1, $G_{x\theta} = G_{\theta z} = G_{xz}$ = 4.3, and Poisson's ratio $\nu_{x\theta}$ = 0.300.

Table 5 Range of imperfection sensitivity (negative b)*

R = 1m, $k_1^2 = k_2^2$ = 5/6

	Lateral External Pressure Only			
	R_2/R_1 = 1.10		RT_2/R_1 = 1.05	
	$\bar{z}$	(l/R)	$\bar{z}$	(l/R)
Circumf Reinf†	2.3–269.6	(0.47–5.07)	1.7–1,045	(0.29–7.15)
Axial Reinf‡	>27.0	(>1.6)	>25.0	(>1.1)
Isotropic**	3.4–952.3	(0.58–9.75)	>3.8	(>0.44)
	w/Hydrostatic End Loading			
	R_2/R_1 = 1.10		R_2/R_1 = 1.051	
	$\bar{z}$	(l/R)	$\bar{z}$	(l/R)
Circumf Reinf†	<353.5	(<5.81)	<1,866	(<9.55)
Axial Reinf‡	>13.1	(>1.12)	>14.1	(>0.83)
Isotropic**	<1,081	(<10.39)	All values	(All values)

* For values of $\bar{z} = l^2(c_{11}c_{22} - c_{12}^2)^{1/2}/[R\sqrt{12}(c_{11}c_{22}D_{11}D_{22})^{1/4}]$, examined from 1.0 to 3000.
† Gr/Ep, Circumferential Reinforcement, moduli in GN/m^2: E_x = 9.1, E_θ = 140.0, $G_{x\theta} = G_{\theta z} = G_{xz}$ = 4.3, and Poisson's ratio $\nu_{x\theta}$ = 0.020.
‡ Gr/Ep, Axial Reinforcement, moduli in GN/m^2: E_x = 140.0, E_θ = 9.1, $G_{x\theta} = G_{\theta z} = G_{xz}$ = 4.3, and Poisson's ratio $\nu_{x\theta}$ = 0.300.
** For Isotropic, modulus E = 140.0 GN/m^2, and Poisson's ratio ν = 0.300.

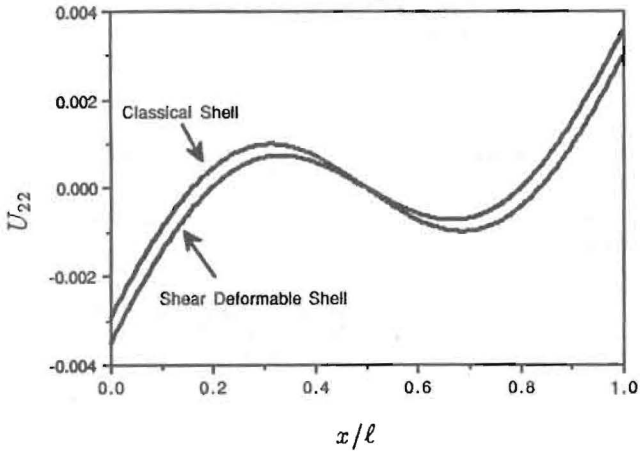

Fig. 4(*a*) $U_{22}(x)$ for both the shear deformable and the classical shell theory (lateral only external pressure)

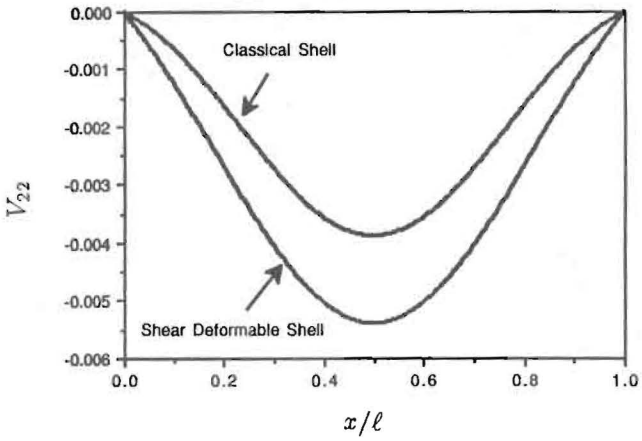

Fig. 4(*b*) $V_{22}(x)$ for both the shear deformable and the classical shell theory

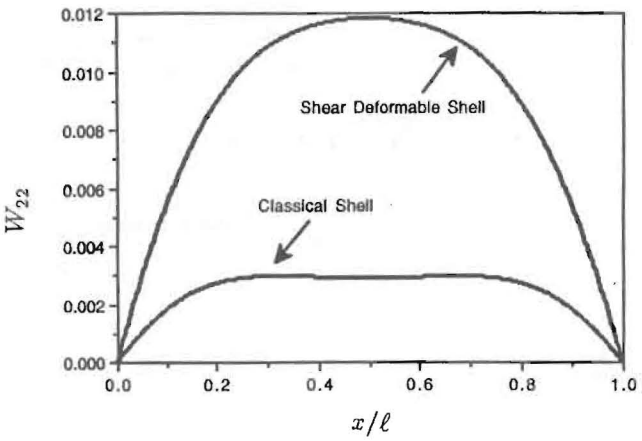

Fig. 4(*c*) $W_{22}(x)$ for both the shear deformable and the classical shell theory

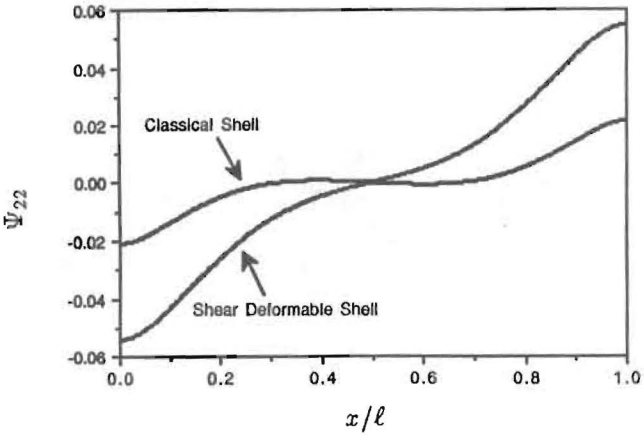

Fig. 4(*d*) $\Psi_{22}(x)$ for both the shear deformable and the classical shell theory

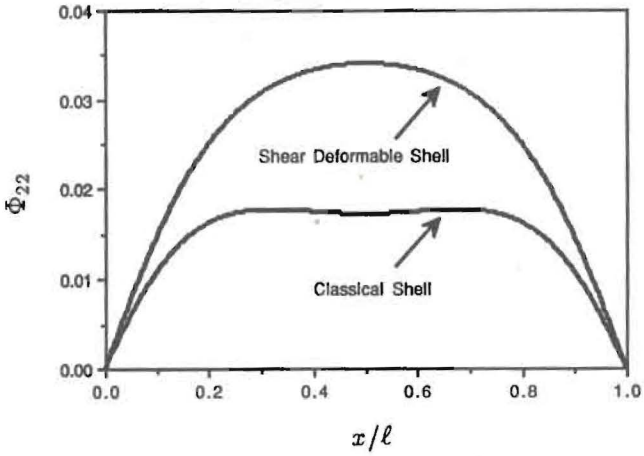

Fig. 4(*e*) $\Phi_{22}(x)$ for both the shear deformable and the classical shell theory

sensitive even at the high range of length values, and therefore reduction in the buckling pressure from the bifurcation values should be anticipated; for the isotropic case, the bifurcation pressure ought to be reliable above $\bar{z} \simeq 1{,}000$. For the rather short shells, i.e., small values of $\bar{z}$, the circumferentially reinforced case shows a large amount of imperfection-sensitivity above $\bar{z} \simeq 2.3$ (and up to $\simeq 270$), whereas the axially reinforced case exhibits no imperfection-sensitivity below $\bar{z} \simeq 27$. One interesting observation from Fig. 1 is that the absolute maximum of the negative range of the postbuckling coefficient, b, is reached in the isotropic case.

Figure 2 and Table 2 give the results for the postbuckling coefficient b from the shear deformable shell theory for the case of hydrostatic end loading. The major changes occur for the rather short shells, i.e., for $\bar{z}$ less than $\simeq 25$, for which the pressure loading of the ends causes an increase of the imperfection sensitivity (smaller values of b) in comparison with the lateral-only external pressure loading.

The results in Table 3 and in Fig. 3 illustrate the effect of transverse shear on the post-buckling coefficient for lateral external pressure loading. Compared to the results from the classical shell theory, i.e., neglecting the transverse shear effects, it can be concluded that this effect leads to a decrease in the value of b and hence increases the imperfection sensitivity of the shell; however, this effect is negligible for longer shells, specifically for $\bar{z}$ above $\simeq 100$.

The effect of thickness is illustrated in Table 4, in which two cases of thickness are considered, a relatively thinner shell with $R_2/R_1 = 1.05$, and a relatively thicker shell with $R_2/R_1 = 1.10$. The shells have the same mean radius $R = 1$ m. Since the Batdorf number $\bar{z}$ depends on the shell thickness, it seems advisable to use the length ratio l/R for comparison purposes in this table. One main point is that for the same length, the thinner and thicker shells may buckle at different values of n. If the shells buckle at the same n (these cases are denoted by an asterisk in the data in Table 4), then it can be concluded that the values of the post-buckling coefficient are larger for the thicker shell and therefore, the thicker shell is less sensitive to imperfections. However, if at the same length, the thicker shell buckles at a smaller n, then b can be smaller and the thicker

shell can be more imperfection-sensitive. Therefore, the thicker shells are less sensitive to imperfections only if they buckle at the same value of n as the thinner shells (of the same length, l, and mean radius, R) with which they are compared.

One of the most useful data in this problem of a shell under external pressure, is the range of imperfection sensitivity, expressed in terms of the range of values of $\bar{z}$, or equivalently, the range of values of l/R, for which the post-buckling coefficient b is negative, and these data are given in Table 5. A range of $\bar{z}$ from 1 to 3,000 was examined. As can be seen, the range of imperfection sensitivity depends on the material anisotropy, the thickness and whether the end pressure loading is included or not. For example, the isotropic case with hydrostatic end loading is always imperfection-sensitive for $R_2/R_1 = 1.05$, but not for the thicker $R_2/R_1 = 1.10$, in which case it shows a positive b and hence lack of imperfection-sensitivity for $\bar{z}$ above $\simeq 1{,}100$.

Finally, in order to illustrate the effect of transverse shear on the second-order displacement field, Figs. 4*a–e* show the functions $U_{22}(x)$, $V_{22}(x)$, $W_{22}(x)$, $\Psi_{22}(x)$, and $\Phi_{22}(x)$ for both the shear deformable and the classical shell theory. The case selected was lateral only external pressure, graphite/epoxy with circumferential reinforcement, radii ratio $R_2/R_1 = 1.10$, and length parameter $\bar{z} = 10$. For this case the structure is imperfection-sensitive with calculated $b = -0.2681$ from the shear deformable shell, and $b = -0.1598$ from the classical shell theory.

Long Cylindrical Shell Limit

If we make the assumption of an infinitely long cylinder, we may ignore boundary conditions at the ends of the shell and the solutions to the differential Eqs. (20) may then be sought in the form of periodic functions of the axial coordinate. Specifically,

$$U_{20} = \tilde{U}_{20} \sin 2\lambda x; \quad V_{20} = \tilde{V}_{20} \cos 2\lambda x;$$

$$W_{20} = \tilde{W}^*_{20} + \tilde{W}_{20} \cos 2\lambda x, \tag{29a}$$

$$\Psi_{20} = \tilde{\Psi}_{20} \sin 2\lambda x; \quad \Phi_{20} = \tilde{\Phi}_{20} \cos 2\lambda x. \tag{29b}$$

Then, substituting into the differential Eqs. (20), gives $\tilde{W}^*_{20}$ from

$$(c_{22} + p_c R)\tilde{W}^*_{20} = (b_1 + b_2 + b_3 + b_4)/4, \tag{30a}$$

where the b_i's are given in Eqs. (19) and λ is the buckling mode from (14*c*). Also, $\tilde{V}_{20} = \tilde{\Phi}_{20} = 0$, and $\tilde{U}_{20}$, $\tilde{W}_{20}$, and $\tilde{\Psi}_{20}$ are found from the linear equations:

$$4\lambda^2 R c_{11}\tilde{U}_{20} + 2\lambda c_{12}\tilde{W}_{20} = \left(\frac{c_{12}}{R} n^2 - R c_{11}\lambda^2\right)\frac{W_1^2\lambda}{4}, \tag{30b}$$

$$2k_1^2 c_{55}\lambda\tilde{W}_{20} - (4D_{11}\lambda^2 + k_1^2 c_{55})\tilde{\Psi}_{20} = 0, \tag{30c}$$

$$2\lambda c_{12} R\tilde{U}_{20} + [c_{22} + p_c R + (k_1^2 c_{55} + N^c_{x0})4\lambda^2 R^2]\tilde{W}_{20} - 2\lambda c_{12} k_1^2 c_{55} R^2 \tilde{\Psi}_{20} = (b_2 + b_4 - b_1 - b_3)/4. \tag{30d}$$

In a similar fashion, solutions to the differential Eqs. (21) are set in the form

$$U_{22} = \tilde{U}_{22} \sin 2\lambda x; \quad V_{22} = \tilde{V}^*_{22} + \tilde{V}_{22} \cos 2\lambda x;$$

$$W_{22} = \tilde{W}^*_{22} + \tilde{W}_{22} \cos 2\lambda x, \tag{31a}$$

$$\Psi_{22} = \tilde{\Psi}_{22} \sin 2\lambda x; \quad \Phi_{22} = \tilde{\Phi}^*_{22} + \tilde{\Phi}_{22} \cos 2\lambda x. \tag{31b}$$

Then, substituting into (21), gives $\tilde{V}^*_{22}$, $\tilde{W}^*_{22}$, and $\tilde{\Phi}^*_{22}$ from

$$\left(\frac{c_{22}}{R} 4n^2 + p_c\right)\tilde{V}^*_{22} + \left(\frac{c_{22}}{R} + p_c\right)2n\tilde{W}^*_{22} = \left(c_{12}\lambda^2 - \frac{c_{22}}{R^2} n^2\right)\frac{W_1^2 n}{4}, \tag{32a}$$

$$2nk_2^2 c_{44}\tilde{W}^*_{22} - \left(\frac{D_{22}}{R} 4n^2 + R k_2^2 c_{44}\right)\tilde{\Phi}^*_{22} = 0, \tag{32b}$$

$$(c_{22} + p_c R)2n\tilde{V}^*_{22} + [(k_2^2 c_{44} + N^c_{\theta 0})4n^2 + c_{22} + p_c R]\tilde{W}^*_{22} - 2nRk_2^2 c_{44}\tilde{\Phi}^*_{22} = (b_3 + b_4 - b_1 - b_2)/4. \tag{32c}$$

Also, $\tilde{U}_{22}$, $\tilde{V}_{22}$, $\tilde{W}_{22}$, $\tilde{\Psi}_{22}$, and $\tilde{\Phi}_{22}$ are found from the linear equations:

$$4\left(R c_{11}\lambda^2 + \frac{c_{66}}{R} n^2\right)\tilde{U}_{22} + 4\lambda n(c_{12} + c_{66})\tilde{V}_{22} + 2\lambda\tilde{W}_{22} = \left(\frac{c_{12} + 2c_{66}}{R} n^2 + R c_{11}\lambda^2\right)\frac{W_1^2\lambda}{4}, \tag{33a}$$

$$4\lambda n(c_{12} + c_{66})\tilde{U}_{22} + \left(\frac{c_{22}}{R} 4n^2 + 4\lambda^2 R c_{66} + p_c\right)\tilde{V}_{22} + 2n\left(\frac{c_{22}}{R} + p_c\right)\tilde{W}_{22} = \left[(c_{12} + 2c_{66})\lambda^2 + \frac{c_{22}}{R^2} n^2\right]\frac{W_1^2 n}{4}, \tag{33b}$$

$$2\lambda k_1^2 c_{55} R\tilde{W}_{22} - \left(\frac{D_{66}}{R} 4n^2 + R k_1^2 c_{55} + 4\lambda^2 R D_{11}\right)\tilde{\Psi}_{22} - 4\lambda n(D_{12} + D_{66})\tilde{\Phi}_{22} = 0, \tag{33c}$$

$$2nk_2^2 c_{44}\tilde{W}_{22} - 4\lambda n(D_{12} + D_{66})\tilde{\Psi}_{22} - \left(4\lambda^2 R D_{66} + \frac{D_{22}}{R} 4n^2 + R k_2^2 c_{44}\right)\tilde{\Phi}_{22} = 0, \tag{33d}$$

$$2\lambda c_{12} R\tilde{U}_{22} + 2n(c_{22} + p_c R)\tilde{V}_{22} + [(k_2^2 c_{44} + N^c_{\theta 0})4n^2 + c_{22} + p_c R + (k_1^2 c_{55} + N^c_{x0})4\lambda^2 R^2]\tilde{W}_{22} - 2\lambda k_1^2 c_{55} R^2\tilde{\Psi}_{22} - 2nRk_2^2 c_{44}\tilde{\Phi}_{22} = (b_4 + b_1 - b_2 - b_3)/4. \tag{33e}$$

The post-buckling coefficient b can now be calculated by substituting into the full expressions for the displacement field, Eqs. (18), and then into the formulas (9) and (10). This closed-form solution for the second-order displacement field for a very long cylindrical shell, besides being a useful quickly obtainable solution, can be used as the initial guess for the relaxation method which is employed to solve the differential equations for the second-order displacements for a cylindrical shell of finite length.

A comparison of this long shell limit solution for the post-buckling coefficient, b, is given in Fig. 5(*a*) for the graphite/epoxy shell with circumferential reinforcement and in Fig. 5(*b*) for the the graphite/epoxy shell with axial reinforcement (lateral external pressure only and $R_2/R_1 = 1.10$). In both cases, the long shell limit essentially converges to the solution outlined in the previous sections for a shell of finite length, when the length values become large, i.e., in the first case for $\bar{z}$ beyond about 100 and the second case for $\bar{z}$ beyond about 400.

Conclusions

1 Koiter's general post-buckling theory is used to study the initial post-buckling behavior of moderately thick, orthotropic, shear deformable cylindrical shells under external pressure. A

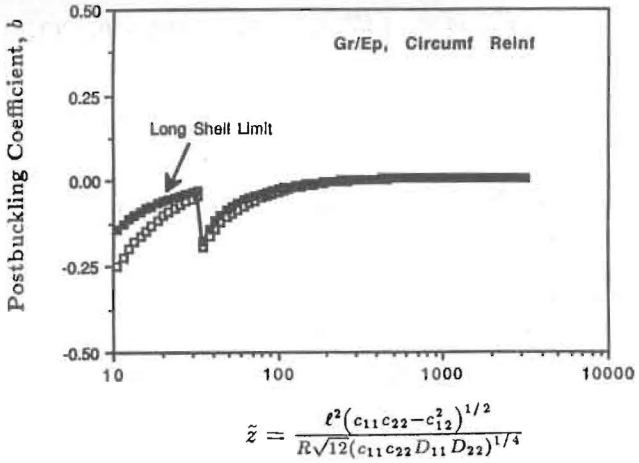

$$\tilde{z} = \frac{\ell^2\left(c_{11}c_{22}-c_{12}^2\right)^{1/2}}{R\sqrt{12}\left(c_{11}c_{22}D_{11}D_{22}\right)^{1/4}}$$

Fig. 5(*a*) The long cylinder limit closed-form solution for the initial postbuckling coefficient, b, in comparison to the finite length solution for a graphite/epoxy with circumferential reinforcement

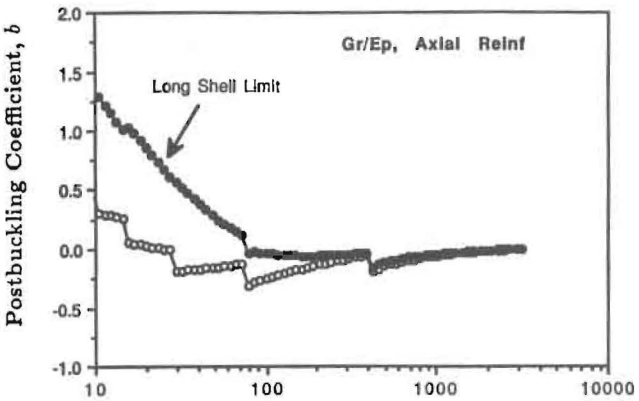

$$\tilde{z} = \frac{\ell^2\left(c_{11}c_{22}-c_{12}^2\right)^{1/2}}{R\sqrt{12}\left(c_{11}c_{22}D_{11}D_{22}\right)^{1/4}}$$

Fig. 5(*b*) The long cylinder limit closed-form solution for the initial postbuckling coefficient, b, in comparison to the finite length solution for a graphite/epoxy with axial reinforcement

shear deformation theory, which accounts for transverse shear strains and rotations about the normal to the shell midsurface, is employed to formulate the shell equations.

2 The range of imperfection sensitivity depends strongly on the material anisotropy, on the wall thickness, and on whether the end pressure loading is included or not.

3 For the circumferentially reinforced graphite/epoxy example case studied, it was found that the structure is not sensitive to imperfections for values of the Batdorf length parameter $\tilde{z}$ above $\simeq$270, whereas for the axially reinforced case the structure is imperfection-sensitive even at the high range of length values; for the isotropic case, the structure is not sensitive to imperfections above $\tilde{z} \simeq 1000$.

4 For the same length, a thicker shell is less sensitive to imperfections if it buckles at the same number of wave numbers (n, m) as the thinner construction.

5 Transverse shear effects lead to an increase in the imperfection sensitivity of the shell; however, this effect is significant only for relatively short shells.

6 If the hydrostatic pressure loading of the ends is included, major changes would occur for rather short shells, for which an increase of the imperfection sensitivity is observed in comparison to the lateral only external pressure loading.

7 A closed-form long-shell limit solution for the initial postbuckling coefficient, b, is derived and shown to properly converge to the solution for a shell of finite length, when the values of $\tilde{z}$ become large.

Acknowledgment

The financial support of the Office of Naval Research, Ship Structures and Systems, S&T Division, Grant N00014-91-J-1892, and the interest and encouragement of the Grant Monitor, Dr. Y. D. S. Rajapakse, are both gratefully acknowledged.

References

Budiansky, B., 1974, "Theory of Buckling and Post-Buckling Behavior of Elastic Structures," *Advances in Applied Mechanics,* Vol. 14, pp. 1–65.

Budiansky, B., and Amazigo, J. C., 1968, "Initial Post-buckling Behavior of Cylindrical Shells Under External Pressure," *Journal of Mathematics and Physics,* Vol. 47, No. 3, pp. 223–235.

Budiansky, B., and Hutchinson, J. W., 1964, "Dynamic Buckling of Imperfection-Sensitive Structures," *Proceedings XI International Congress of Applied Mechanics,* H. Görtler, ed, Springer, Munich, pp. 636–651.

Brush, D. O., and Almroth, B. O., 1975, *Buckling of Bars, Plates, and Shells,* McGraw-Hill, New York, pp. 159–161.

Dong, S. B., and Nelson, R. B., 1972, "On Natural Vibrations and Waves in Laminated Orthotropic Plates," ASME JOURNAL OF APPLIED MECHANICS, Vol. 39, pp. 739–745.

Dong, S. B., and Tso, F. K. W., 1972, "On a Laminated Orthotropic Shell Theory Including Transverse Shear Deformation," ASME JOURNAL OF APPLIED MECHANICS, Vol. 39, pp. 1091–1097.

Fu, L., and Waas, A. M., 1995, "Initial Post-buckling Behavior of Thick Rings Under Uniform External Hydrostatic Pressure," ASME JOURNAL OF APPLIED MECHANICS, Vol. 62, pp. 338–345.

Hutchinson, J. W., 1968, "Buckling and Initial Postbuckling Behavior of Oval Cylindrical Shells Under Axial Compression," ASME JOURNAL OF APPLIED MECHANICS, Vol. 35, pp. 66–72.

Hutchinson, J. W., and Frauenthal, J. C., 1969, "Elastic Postbuckling Behavior of Stiffened and Barreled Cylindrical Shells," ASME JOURNAL OF APPLIED MECHANICS, Vol. 36, pp. 784–790.

Hutchinson, J. W., and Koiter, W. T., 1970, "Postbuckling theory," ASME *Appl. Mech. Rev.* Vol. 23, pp. 1353–1366.

Kardomateas, G. A., 1993, "Buckling of Thick Orthotropic Cylindrical Shells Under External Pressure," ASME JOURNAL OF APPLIED MECHANICS, Vol. 60, 1993, pp. 195–202.

Kardomateas, G. A., and Chung, C. B., 1994, "Buckling of Thick Orthotropic Cylindrical Shells Under External Pressure Based on Non-Planar Equilibrium Modes," *International Journal of Solids and Structures,* Vol. 31, No. 16, pp. 2195–2210.

Kardomateas, G. A., and Philobos, M. S., 1995, "Buckling of Thick Orthotropic Cylindrical Shells Under Combined External Pressure and Axial Compression," *AIAA Journal,* Vol. 33, No. 10, pp. 1946–1953.

Koiter, W. T., 1945, *On the Stability of Elastic Equilibrium* (in Dutch), thesis, Delft, Amsterdam; English transl. (a) NASA TT-F10, 833 (1967), (b) AFFDL-TR-70-25 (1970).

Koiter, W. T., 1956, "Buckling and Postbuckling Behavior of a Cylindrical Panel Under Axial Compression," NLR Rep. No. S476. Rep. Trans. Nat. Aero. Res. Inst. Vol. 20, Nat. Aero. Res. Inst., Amsterdam.

Koiter, W. T., 1963, "Elastic Stability and Post-Buckling Behavior," *Non-Linear Problems,* R. E. Langer ed., University of Wisconsin Press, Madison, WI.

Mindlin, R. D., 1951, "Influence of Rotatory Inertia and Shear on Flexural Motions in Isotropic Elastic Plates" ASME JOURNAL OF APPLIED MECHANICS, Vol. 18, pp. 31–38.

Mirsky, I., and Herrmann, G., 1957, "Nonaxially symmetric motion of cylindrical shells," *J. Acoust. Soc. Am.,* Vol. 29, pp. 1116–1123.

Naghdi, P. M., and Cooper, R. M., 1956, "Propagation of elastic waves in cylindrical shells including the effects of transverse shear and rotatory inertia," *J. Acoust. Soc. Am.* Vol. 28, pp. 56–63.

Nemeth, M. P., 1994, "Nondimensional Parameters and Equations for Buckling of Anisotropic Shallow Shells," ASME JOURNAL OF APPLIED MECHANICS, Vol. 61, pp. 664–669.

Press, W. H., Flannery, B. P., Teukolsky, S. A., and Vetterling, W. T., 1989, *Numerical Recipes,* Cambridge University Press, Cambridge, UK.

Reddy, J. N., and Liu, C. F., 1985, "A Higher-Order Shear Deformation Theory of Laminated Elastic Shells," *Int. J. Eng. Sci.,* Vol. 23, No. 3, pp. 319–330.

Sheinman, I., and Simitses, G. J., 1983, "Buckling and Postbuckling of Imperfect Cylindrical Shells Under Axial Compression," *Computers & Structures,* Vol. 17, No. 2, pp. 277–285.

Simitses, G. J., Tabiei, A., and Anastasiadis, J. S., 1993, "Buckling of Moderately Thick, Laminated Cylindrical Shells Under Lateral Pressure," *Composites Engineering,* Vol. 3, No. 5, pp. 409–417.

Whitney, J. M., 1973, "Shear Correction Factors for Orthotropic Laminates Under Static Load," ASME JOURNAL OF APPLIED MECHANICS, Vol. 40, pp. 302–304.

Whitney, J. M., and Sun, C. T., 1974, "A Refined Theory for Laminated Anisotropic Cylindrical Shells," ASME JOURNAL OF APPLIED MECHANICS, Vol. 41, pp. 471–476.